Journal of Environmental Chemical Engineering 7 (2019) 102800

Contents lists available at ScienceDirect

Journal of Environmental Chemical Engineering

journal homepage: www.elsevier.com/locate/jece

A new synthetic antifouling coatings integrated novel aminothiazole-functionalized ionic liquids motifs with enhanced antibacterial performance

Reda F.M. Elshaarawy[a,b,*], Fatma H.A. Mustafa[c], Ahmed R. Sofy[d], Ahmed A. Hmed[d], Christoph Janiak[a]

[a] Institut für Anorganische Chemie und Strukturchemie, Heinrich-Heine Universität Düsseldorf, 40204 Düsseldorf, Germany
[b] Faculty of Science, Suez University, Suez, Egypt
[c] National Institute of Oceanography and Fisheries, Marine chemistry Laboratory, Marine Environment Division, Suez, Egypt
[d] Botany and Microbiology Department, Faculty of Science, Al-Azhar University, 11884 Nasr City, Cairo, Egypt

ARTICLE INFO

Keywords:
Biofouling
Aminothiazoles
Ionic liquid
Antibacterial
Antifouling coatings

ABSTRACT

Prohibition of using the organotin-based antifouling coatings by International Maritime Organization (IMO), due to their serious environmental and health impacts, open a new avenue of a challenge for many researchers to search for new tin-free additives for antifouling coatings. In addressing this challenge, we have successfully prepared new ionic liquids-based salicylidene-iminothiazole and benzylidene-bis-iminothiazole Schiff bases (SITSB and BBITSB) to explore their antibacterial and antifouling performances. These novels Schiff bases manifested moderate to excellent broad-spectrum antibacterial efficacy against most common marine biofilm-inducing bacteria. Moreover, incorporation of these bactericidal Schiff bases into the matrix of inert commercial paints has significantly enhanced their antifouling performance as revealed from the field-static immersion study in the Mediterranean. In summary, structural refinement of these aminothiazole Schiff bases along with extensive environmental and toxicity assessments may offer a new generation of promising antifouling additives.

1. Introduction

Marine biofouling, a worldwide problem in marine ecosystems leads to undesirable negative economic and environmental impacts [1], is the adhesion and accumulation of various marine organisms (*e.g.* microbial slimes, macro-algae, tube worms and barnacles) on marine substructure surfaces. Throughout the world, more than 4000 marine biofouling-inducing organisms have been recognized [2]. Among these biofouling-inducing organisms, bacteria act as the key microfoulant in biofouling process progress. Where the adhesion of bacteria to any submerged structures (such as ship hulls, pipelines, heat exchangers, *etc*.) results in bacterial communities enclosed in a polymeric matrix which is called a bacterial biofilm [3]. Wherever this biofilm is formed, numerous problems have been developed. The overall negative economic impacts of biofouling are the expenditures and time consumed to remove it [4].

In addressing the above challenges, extensive researches have been carried out for exploring innovative marine antifouling (AF) strategies. These earlier studies have resulted in the development of diverse AF systems over last decades starting from copper and lead sheathing to copper, lead, arsenic and mercury biocides-based AF coatings, by the 20th century. The real revolution in AF coatings was started in the 1950s when organotin-based AF coatings were developed due to their improved wide-range activity, the absence of corrosion effects and their acceptable colour. Concurrently, using of organotin derivatives in AF systems has remarkably grown in a short time due to their promoted biological activities along with enhanced mechanical properties. Nevertheless, their serious environmental impacts have pushed the European countries to restrict their further application and have banned their using worldwide in 2008 [5]. Thus, there is existing challenge and urgent need to explore new effective and environmentally safe organotin alternatives having higher efficacies to hinder biofilm formation and consequently, diminish the biofouling process. Recently, AF-interested researchers are focused on the suppression of bacterial and diatoms adhesion to submerged surfaces that to hinder the biofilm formation as it is a pivotal step in biofouling process.

The widespread therapeutic applications of thiazole derivatives such as antibacterial [6], anti-fungal [6], anti-cancer [7], anti-tumor [8], anti-diabetic [9], anti-viral [10], CNS depressant [11], anti-oxidant [12], anti-filarial [13], and anthelmintic [14] make them supreme templates for constructing novel chemotherapeutic and biological agents. Moreover, aminothiazole Schiff bases, in particular, are of

* Corresponding author at: Institut für Anorganische Chemie und Strukturchemie, Heinrich-Heine Universität Düsseldorf, 40204 Düsseldorf, Germany.
E-mail addresses: reel-001@hhu.de, reda.elshaarawy@suezuniv.edu.eg (R.F.M. Elshaarawy).

https://doi.org/10.1016/j.jece.2018.11.044
Received 3 April 2018; Received in revised form 19 November 2018; Accepted 21 November 2018
Available online 23 November 2018

significant concern for their powerful anti-cancer [15], anti-microbial [16] and antifungal [17] activities. Interestingly that imidazolium and pyridinium ionic liquids (ILs) terminals are remarkably enhanced the anti-microbial [18], anti-cancer [19], anti-algale and anti-adhesive efficacies [20] of biological molecules.

Inspired by the aforementioned remarks and with sustainability for our program interested in the fabrication of novel biological [21] and AF candidates [22,21c], in this work we have selected 2-aminothiazole (2-AT) as a template to construct a series of novel IL-based 2-AT Schiff bases to investigate their antibacterial and antibiofouling behaviours with emphasis to build up a new generation of marine-safe and tin-free antibiofoulants alternatives.

2. Experimental section

2.1. Materials

(See supplementary information)

2.2. Instrumentation

(See supplementary information)

2.3. Synthesis

2.3.1. Salicylaldehydes ionic liquids (Sal-ILs)

(See supplementary information)

2.3.2. Synthesis of 2-aminothiazole Schiff bases

Generally, a mixture of an ethanolic solution (50 mL) containing (3.00 g, 30 mmol) of 2-AT and (30 mmol) of salicylaldehydes (**1b,c**) or salicylaldehyde ionic liquids, Sal-ILs, (**3a-e**) into a 100 mL RB flask was refluxed for 2–6 h (the reaction progress was monitored by TLC). After completion of the reaction, the reaction mixture was cooled to room temperature giving a solid product after 30 min, which was filtered, washed with ethanol (3 × 3 mL), ether (3 × 3 mL), dried and then recrystallized from ethanol. Samples of the isolated products **(4a,b, 5a-e)** were characterized as follows;

2.3.2.1. 2-(3-methoxysalicylidene)-iminothiazole (4a). Reddish brown crystals, 85% yield (5.97 g), mp = 115–116 °C. FTIR (KBr, cm^{-1}) 3410 (*vs*, br, ν(O—H)), 3056 (m, br, $\nu_{asym(C-H)}$, Ar), 3005 (m, br, $\nu_{sym(C-H)}$, Ar), 1621 (s, sh, ν(C=N), azomethine), 1591 (w, br, ν(C=N), thiazole ring), 1461, 1371 (w, br, ν(C=C)), 1274 (m, sh, $\nu_{(Ar-O)}$), 1239 (m,sh), 1141 (m, sh, $\nu_{(C-N-C)}$), 962 (w, br, ν(C—S—C)$_{str}$), 725 (m, br, ν(C—S—C)$_{bend}$). ^{1}H NMR (300 MHz, DMSO-d_6) δ (ppm) 11.36 (s, 1 H), 9.32 (s, 1 H), 7.74 (d, *J* = 3.49 Hz), 7.65 (d, *J* = 3.49 Hz), 7.43 (dd, *J* = 1.44, 7.95 Hz), 7.19 (dd, *J* = 1.47, 8.02 Hz, 1 H), 6.93 (t, *J* = 7.94 Hz, 1 H), 3.84 (s, 3 H). ^{13}C NMR (125 MHz, DMSO-d_6) δ (ppm) 171.30, 163.99, 150.63, 148.53, 141.97, 122.88, 120.07, 120.02, 119.79, 116.90 and 56.41. EI–MS, *m/z* (%): 234.1 (58.60) ($[C_{11}H_{10}N_2O_2S]^+$, M). Anal. calcd for $C_{11}H_{10}N_2O_2S$ (M = 234.27) C, 56.39; H, 4.30; N, 11.96; S, 13.69%, found C, 56.19; H, 4.42; N, 11.68; S, 13.55%.

2.3.2.2. 2-(3-ethoxysalicylidene)-iminothiazole (4b). Canary yellow powder, 96% yield (7.15 g), mp = 119–120 °C. FTIR (KBr, cm^{-1}) 3426 (vs, br, ν(O—H)), 3116 (m, br, $\nu_{asym(C-H)}$, Ar), 3064 (m, br, $\nu_{sym(C-H)}$, Ar), 1618 (s, sh, ν(C=N), azomethine), 1593 (w, br, ν(C=N), thiazole ring), 1470, 1390 (w, br, ν(C=C)), 1272 (m, sh, $\nu_{(Ar-O)}$), 1240 (m,sh), 1139 (m, sh, $\nu_{(C-N-C)}$), 1005 (w, br, ν(C—S—C)$_{str}$), 726 (m, br, ν(C—S—C)$_{bend}$). ^{1}H NMR (300 MHz, DMSO-d_6) δ (ppm) 10.11 (s, 1 H), 9.19 (s, 1 H), 8.19 (s, 2 H), 8.07 (d, *J* = 8.3 Hz, 1 H), 7.84– 7.68 (m, 2 H), 3.44 (qd, *J* = 7.0, 5.1 Hz, 2 H), 3.44 (t, *J* = 7.0 Hz, 3 H). ^{13}C NMR (125 MHz, DMSO-d_6) δ (ppm) 172.32, 163.47, 163.39, 142.28, 138.66, 131.57, 130.53, 130.40, 123.64, 120.78, 56.49 and 19.03. EI–MS, *m/z* (%) 248.2 (66.16) ($[C_{12}H_{12}N_2O_2S]^+$, M). Anal. calcd for $C_{12}H_{12}N_2O_2S$ (M = 248.30): C, 58.05; H, 4.87; N, 11.28; S, 12.91%, found C, 57.89; H, 4.93; N, 11.19; S, 12.75%.

2.3.2.3. 2-(5-(2-methylpyridinium chloride)-salicylidene))-iminothiazole (5a). Reddish brown powder, 60% yield (6.23 g), mp = over 300 °C. FTIR (KBr, cm^{-1}) 3386 (vs, br, ν(O—H)), 3086 (m, br, $\nu_{asym(C-H)}$, Ar), 3001 (m, br, $\nu_{sym(C-H)}$, Ar), 1617 (s, sh, ν(C=N), azomethine), 1569 (w, br, ν(C=N), thiazole ring), 1511, 1444, 1383 (s, sh, ν(C=C)), 1274 (m, sh, $\nu_{(Ar-O)}$), 1243 (m,sh), 1149 (m, sh, $\nu_{(CN_C)}$), 1081 (w, br, ν(C—S—C)$_{str}$), 700 (m, br, ν(C—S—C)$_{bend}$). ^{1}H NMR (500 MHz, DMSO-d_6) δ (ppm) 10.28 (s, 1 H), 9.80 (s, 1 H), 8.73 (s, 1 H), 8.68-8.63 (m, 1 H), 8.19 (t, *J* = 8.03 Hz, 1 H), 7.71-7.59 (m, 2 H), 7.55-7.43 (m, 1 H), 7.21 (d, *J* = 4.16 Hz, 1 H), 7.13-7.02 (m, 1 H), 6.84 (d, *J* = 4.22 Hz, 1 H), 5.43 (s, 2 H), 3.18 (s, 3 H). ^{13}C NMR (125 MHz, DMSO-d_6) δ (ppm) 172.99, 157.00, 153.79, 150.57, 147.83, 144.29, 140.31, 134.36, 131.66, 129.60, 126.38, 123.41, 122.57, 117.42, 108.06, 55.32 and 21.40. ESI-MS, *m/z* 311.4 ($[C_{17}H_{16}N_3OS]^+$, M - Cl^-). Anal. calcd for $C_{17}H_{16}ClN_3OS$ (M = 345.85) C, 59.04; H, 4.66; N, 12.15; S, 9.27%, found C, 58.96; H, 4.78; N, 12.11; S, 9.13%.

2.3.2.4. 2-(5-(1-ethyl-imidazol-3-ium chloride)-salicylidene))-iminothiazole (5b). Reddish brown powder, 96% yield (6.93 g), mp = over 300 °C. FTIR (KBr, cm^{-1}) 3434 (vs, br, ν(O—H)), 3092 (m, br, $\nu_{asym(C-H)}$, Ar), 3063 (m, br, $\nu_{sym(C-H)}$, Ar), 1621 (s, sh, ν(C=N), azomethine), 1591 (w, br, ν(C=N), thiazole ring), 1516, 1448, 1385 (s, sh, ν(C=C)), 1276 (m, sh, $\nu_{(Ar-O)}$), 1238 (m,sh), 1155 (m, sh, $\nu_{(C-N_C)}$), 1053 (w, br, ν(C—S—C)$_{str}$), 739 (m, br, ν(C—S—C)$_{bend}$). ^{1}H NMR (500 MHz, DMSO-d_6) δ (ppm) 10.36 (s, 1 H), 9.48 (s, 1 H), 9.38 (s, br, 1 H), 8.68 (d, *J* = 1.74 Hz, 1 H), 7.85-7.70 (m, 2 H), 7.45 (d, *J* = 1.71 Hz, H), 7.28-7.18 (m, 2 H), 7.04-6.91 (m, H), 5.45 (s, 2 H), 4.22 (dq, *J* = 5.83, 7.30 Hz, 2 H), 1.46 (t, *J* = 8.28, 3 H). ^{13}C NMR (125 MHz, DMSO-d_6) δ (ppm) 167.54, 154.44, 140.27, 136.10, 135.72, 129.09, 122.93, 122.62, 121.60, 118.55, 116.21, 112.88, 56.93, 43.14 and 15.97. ESI-MS, *m/z* 313.5 ($[C_{16}H_{17}N_4OS]^+$, M − Cl^-). Anal. calcd for $C_{16}H_{17}ClN_4OS$ (M = 348.85) C, 55.09; H, 4.91; N, 16.06; S, 9.19%, found C, 55.03; H, 4.98; N, 15.98; S, 9.11%.

2.3.2.5. 2-(5-(1,2-dimethyl-imidazol-3-ium chloride)-salicylidene))-iminothiazole (5c). Orange powder, 96% yield (3.33 g), mp = over 300 °C. FTIR (KBr, cm^{-1}) 3420 (vs, br, ν(O—H)), 3068 (m, br, $\nu_{asym(C-H)}$, Ar), 3031 (m, br, $\nu_{sym(C-H)}$, Ar), 1619 (s, sh, ν(C=N), azomethine), 1587 (w, br, ν(C=N), thiazole ring), 1514 (vs, sh, ν(C=C)), 1452, 1381 (w, br, ν(C=C)), 1270 (m, sh, $\nu_{(Ar-O)}$), 1239 (m,sh), 1153 (m, sh, $\nu_{(C-N-C)}$), 1044 (w, br, ν(C—S—C)$_{str}$), 746 (m, br, ν(C—S—C)$_{bend}$). ^{1}H NMR (500 MHz, DMSO-d_6) δ (ppm) 10.80 (s, 1 H), 9.87 (s, 1 H), 8.15 (d, *J* = 1.79 Hz, 1 H), 7.85-7.50 (m, 2 H), 7.43 (d, *J* = 1.68 Hz, 1 H), 7.15-6.89 (m, 1 H), 5.42 (s, 2 H), 3.73 (s, 3 H), 2.61 (s, 3 H). ^{13}C NMR (125 MHz, DMSO-d_6) δ (ppm) 190.16, 165.51, 161.32, 158.21, 136.23, 128.64, 125.76, 123.28, 121.36, 118.48, 117.78, 57.63, 39.56 and 11.78. ESI-MS, *m/z* 513.5 ($[C_{16}H_{17}N_4OS]^+$, M – Cl^-). Anal. calcd for $C_{16}H_{17}ClN_4OS$ (M = 348.85) C, 55.09; H, 4.91; N, 16.06; S, 9.19%, found C, 54.98; H, 5.02; N, 15.88; S, 9.01%.

2.3.2.6. -(5-(1,2-dimethyl-imidazol-3-ium chloride)-3-methoxysalicylidene))-iminothiazole (5d). Dark red powder, 98% yield (7.94 g), mp = decomposed over 300 °C. FTIR (KBr, cm^{-1}) 3417 (vs, br, ν(O—H)), 3102 (m, br, $\nu_{asym(C-H)}$, Ar), 3056 (m, br, $\nu_{sym(C-H)}$, Ar), 1611 (s, sh, ν(C=N), azomethine), 1571 (w, br, ν(C=N), thiazole ring), 1512 (vs, sh, ν(C=C)), 1462, 1383 (w, br, ν(C=C)), 1290 (m, sh, $\nu_{(Ar-O)}$), 1243 (m,sh), 1150 (m, sh, $\nu_{(C-N-C)}$), 1068 (w, br, ν(C—S—C)$_{str}$), 743 (m, br, ν(C—S—C)$_{bend}$). ^{1}H NMR (500 MHz, DMSO-d_6) δ (ppm): 9.11 (s, 1 H), 8.90 (s, 1 H), 8.78 (s, br, 1 H), 7.67-7.61 (m, 1 H), 7.64-7.56 (m, 1 H), 7.29 (s, 1 H), 7.19 (d, *J* = 11.23 Hz, 1 H), 7.09 (s, 1 H), 5.25 (s, 2 H), 3.85 (s, 3 H), 3.18 (s, 3 H), 2.47 (s, 3 H). ^{13}C NMR (125 MHz, DMSO-d_6) δ (ppm) 175.52, 162.45, 159.42, 157.12, 147.28,

144.78, 130.45, 125.65, 123.14, 121.33, 118.67, 105.44, 101.69, 56.08, 51.21, 25.99 and 10.79. ESI-MS, *m/z* 343.3 ($[C_{17}H_{19}N_4O_2S]^+$, M − Cl^-). Anal. calcd for $C_{17}H_{19}ClN_4O_2S$ (M = 378.88) C, 53.89; H, 5.05; N, 14.79; S, 8.46%, found C, 53.78; H, 5.11; N, 14.71; S, 8.31%.

2.3.2.7. -(5-(1,2-dimethyl-imidazol-3-ium chloride)-3-ethoxysalicylidene))-iminothiazole (5e). Brown powder, 87% yield (7.31 g), mp = decomposed over 300 °C. FTIR (KBr, cm^{-1}) 3381 (vs, br, ν(O—H)), 3180 (m, br, $\nu_{asym(C-H)}$, Ar), 3087 (m, br, $\nu_{sym(C-H)}$, Ar), 1606 (s, sh, ν(C═N), azomethine), 1564 (w, br, ν(C═N), thiazole ring), 1506 (vs, sh, ν(C═C)), 1474, 1391 (w, br, ν(C═C)), 1274 (m, sh, $\nu_{(Ar-O)}$), 1240 (m,sh), 1153 (m, sh, $\nu_{(C-N-C)}$), 1062 (w, br, $\nu(C-S-C)_{str}$), 737 (m, br, $\nu(C-S-C)_{bend}$). ^{1}H NMR (500 MHz, DMSO-d_6) δ (ppm) 10.27 (s, 1 H), 8.91 (s, 1 H), 8.61 (s, br, 1 H), 7.72-7.63 (m, 1 H), 7.37 (d, *J* = 1.85 Hz, 1 H), 7.31-7.23 (m, 1 H), 6.97-6.87 (m, 2 H), 5.34 (s, 2 H), 4.08 (q, 2 H), 3.76 (s, 3 H), 2.67 (s, 3H,), 1.38 (t, *J* = 7.96 Hz, 3 H).^{13}C NMR (125 MHz, DMSO-d_6) δ (ppm) 173.54, 165.27, 151.54, 147.10, 146.76, 141.49, 129.01, 125.80, 122.86, 121.40, 119 119.85, 118.93, 117.82, 65.09, 51.36, 39.44, 14.94 and 9.92. ESI-MS, *m/z* 357.4 ($[C_{18}H_{21}N_4O_2S]^+$, M − Cl^-). Anal. calcd for $C_{18}H_{21}ClN_4O_2S$ (M = 392.90) C, 55.02; H, 5.39; N, 14.26; S, 8.16%, found: C, 55.01; H, 5.39; N, 14.18; S, 8.11%.

2.3.3. Synthesis of N,N'-(1,4-phenylenebis(methan-1-yl-1-ylidene)) dithiazol-2-amine ***(6)***

A mixture of an ethanolic solution (50 mL) containing (3.00 g, 30 mmol) of 2-AT and (2.01 g, 15 mmol) of terephthalaldehyde into a 100 mL RB flask was refluxed for 5 h. After completion of the reaction, the reaction mixture was cooled to room temperature giving a solid product after 15 min, which was filtered, washed with ethanol (3 × 3 mL), ether (3 × 3 mL), dried and then crystallized from ethanol to give compound **6** as a pale yellow powder, 83% yield (3.72 g), mp = 220–221 °C. FTIR (KBr, cm^{-1}): 3091 (m, br, $\nu_{asym(C-H)}$, Ar), 3065 (m, br, $\nu_{sym(C-H)}$, Ar), 1685 (s, sh, ν(C═N), azomethine), 1600 (s, sh, ν(C═N), thiazole ring), 1523 (vs, sh, ν(C═C)), 1483, 1413 (w, br, ν(C═C)), 1236 (m, sh), 1113 (m, sh, $\nu_{(C-N-C)}$), 1011 (w, br, $\nu(C-S-C)_{str}$), 716 (m, br, $\nu(C-S-C)_{bend}$). ^{1}H NMR (500 MHz, DMSO-d_6) δ (ppm) 11.34 (s, 2 H), 9.32 (s, 1 H), 7.75 (d, *J* = 3.48 Hz, 2 H), 7.67 (d, *J* = 3.49 Hz, 2 H), 7.43 (dd, *J* = 1.43, 7.93 Hz, 1 H), 7.19 (dd, *J* = 1.44, 8.03 Hz, 1 H), 6.93 (t, *J* = 7.94 Hz, 1 H). ^{13}C NMR (125 MHz, DMSO-d_6) δ (ppm) 171.08, 164.16, 150.90, 147.57, 141.88, 123.17, 120.02, 119.96, 119.72 and 118.31. EI–MS, *m/z* 298.4 ($[C_{14}H_{10}N_4S_2]^+$, M). Anal. calcd for $C_{14}H_{10}N_4S_2$ (M = 298.39) C, 56.35; H, 3.38; N, 18.78; S, 21.49%, found: C, 56.24; H, 3.41; N, 18.65; S, 21.14%.

2.4. Fabrication of antifouling coatings

The base matrix of the paint consists of a (4:2:1:2:4 w:w:w:w:v) mixture of rosin, chlorinated rubber, iron oxide, dioctyl phthalate (DOP) and xylene. These ingredients were milled together in a high-speed centrifuge ball mill. The milling process was continued until a certain degree of finesse grind was reached. The viscosity was adjusted and the resulting paint formulation was stored in well tight bottles and a cool place. The synthesized compounds were mixed with the prepared paint formulations with a ratio of (1:10 w:w).

2.5. Antibacterial activity against marine biofilm-inducing bacterial strains

2.5.1. Reagents

Dimethylsulphoxide (DMSO) and 3-(3,4-dichlorophenyl)-1,1-dimethylurea (Diuron®, DCMU®) antifoulant ($C_9H_{10}Cl_2N_2O$, 233.09 g mol^{-1}) were obtained from Sigma Chemical Co. (Germany). An indicator solution for determination of bacterial growth of a 70% ethanolic solution of 2-(4-iodophenyl)-3-(4-nitrophenyl)-5-phenyltetrazolium chloride (INT) (2 mg/mL) was purchased from Sigma.

2.5.2. Bacterial cultures

The antibacterial activity of new products was assessed against four marine bacterial species: *Staphylococcus aureus* (*S. aureus,* ATCC 25923) (American Type Culture Collection, Rockville, MD), *Escherichia coli* (*E. coli,* ATCC 25922), *Aeromonas hydrophila* (*A. hydrophila*) and *Vibrio* maintained in BHI at 20 °C. 300 mL of each stock-culture was added to 3 mL of nutrient broth (NB). Then, these cultures were kept for 24 h at 36 ± 1 °C and the purity of these cultures was checked after 8 h of incubation. After 24 h of incubation, bacterial suspension (inoculum) was diluted with a sterilized physiological solution to 10^8 CFU/mL (CFU = Colony Forming Units) (turbidity = McFarland barium sulfate standard 0.5). For the direct bio-autographic test, the bacterial suspension was diluted with brain-heart infusion (BHI) broth to a concentration of ~10^8 CFU/mL (turbidity = McFarland standard 3).

2.5.3. Antimicrobial susceptibility

Antimicrobial susceptibility of the bacterial strains was carried out by agar well diffusion method [23] for the target compounds as well as the standard antifoulant, Diuron®. The diameters of the zone of inhibition (ZOI, mm) were measured accurately as indicative of antimicrobial activity.

2.6. Field anti-macrofouling assay at Alexandria Eastern Harbour beach

2.6.1. Environmental parameters of Alexandria Eastern Harbour waters

In order to optimize the conditions under which the field static antifouling immersion test has been performed, triplicate seawater surface samples were collected from the site of immersion using a Neskin Reversing bottle during immersion period for estimation of the physicochemical parameters. The temperature of seawater was *in situ* measured by an inductive portable thermometer. Salinity was measured by a Bench-portable conductivity meter model Beckman RS-10-X3. Hydrogen-ion concentration (pH-value) of seawater samples was measured using a JENWAY 3410 Electrochemistry Analyzer pH-meter with reading up to 0.01 pH unit taking into consideration certain precautions in the sampling and standardization processes. Dissolved oxygen (DO) was determined by the classical Winkler's method modified by Grasshoff [24]. Oxidizable organic matter (OOM) was quantified by the permanganate oxidation method [25]. The nutrients; ammonia, nitrite, nitrate, phosphate and silicate were determined calorimetrically according to the methods described by Parsons et al. [26] and their absorbance was measured by a UV–vis single beam spectrophotometer (Beckman model DU6) with the range 190–900 nm using 1 cm (matching) cells. Sulphate concentrations were measured turbidimetric according to the earlier described method [27].

2.6.2. Field static immersion antifouling coating test at Alexandria Eastern Harbour

The synthesized aminothiazole Schiff bases (**4**a,b), (**5**a-c) and (**6**) have been undergone a field static immersion antifouling experiment to assess their efficacies in preventing biofouling growth under harsh marine conditions over specific time intervals mainly from spring 2015 to autumn 2015. In this test, seven coating formulations were prepared by incorporating of the synthesized aminothiazole Schiff bases (**4**a,b), (**5**a-c), (**6**) and a standard antifoulant (Diuron®), separately, into the matrix of an inert commercial paint (1 g of the tested compound/10 g of paint). An inert paint formulation was also used as a control. Acrylic panels with dimensions of 10.0 × 15.0 × 0.2 cm were used as bearers for formulated coatings. Emery sand papers with various grades were employed to enhance the roughness of the whole surface for panels. Both of the roughened panels' sides were coated twice with the prepared coating formulations, allowing for a time interval of two days for air-drying between each coating. The coated panels were fixed to the iron frames by nylon threads (see Fig. S1). Triplicate frames were oriented vertically in Alexandria Eastern Harbor seawater at approximately 1.5 m deep where their antifouling performance was followed

by a visual inspection and a photographic recording within a period of 147 days. The AF performance of all coated panels was evaluated by calculating the total cover percentage for different marine fouling organisms over different time intervals.

2.6.3. Statistical analysis

Statistical analysis was performed by (Excel program 2010) using normal fouling cover percentage and seawater physicochemical measurements data in order to determine correlation coefficient (r) and significance (P) for each correlation. P values ≤ 0.05 were considered significant.

3. Results and discussion

3.1. Chemistry

Our synthesis protocol involves two main subsequent stations; initial station designed for fabrication of chlorido picolinium/ imidazolium salicylaldehydes ionic liquids (Sal-ILs) starting from salicylaldehydes *via* an electrophilic aromatic substitution (chloromethylation) reaction to give chloromethyl salicylaldehydes (**2a-c**) which were used as alkylating agents for facile and efficient quaternization of 1,2-dimethylimidazole (1,2-Me_2Im), 2-methylpyridine (2-MePy) or 1-ethylimidazole (1-EtIm) affording the desired products, Sal-ILs (**3a-e**), (see Scheme 1). The Sal-ILs (**3a-e**) were isolated in excellent yields in highly pure states and characterized by elemental and spectral analysis (FTIR, ^{1}H NMR, ^{13}C NMR, ESI-MS). The final station was used for preparation of a novel series of 2-(alkoxysalicylaldimine)-thiazoles Schiff bases (**4a,b**) and 2-(picolinium-/ imidazolium-salicylaldimine)-thiazoles Schiff bases (**5a-e**), respectively *via* Schiff base condensation of equimolar amounts of 2-AT with salicylaldehydes (**1b,c**) and Sal-ILs (**3a-e**) under refluxing conditions in an ethanolic media and catalytic amount of acetic acid (Scheme 1).

Moreover, bis-thiazolo-benzylidendiimine (**6**) was also synthesized by a Schiff base condensation of terephthalaldehyde with 2-AT in 1:2 M ratios. The 2-AT Schiff bases ((**4a,b**), (**5a-e**), **6**) were isolated in excellent yields with highly pure state and characterized by elemental and spectral analysis (FTIR, ^{1}H NMR, ^{13}C NMR, EI/ ESI-MS).

3.2. Structural characterizations of new compounds

3.2.1. Microanalytical and MS data

Elemental analysis for new Schiff bases provided satisfactory data which were in good agreement with their proposed structures (see the experimental section). Moreover, molecular signatures collected from mass spectral data for each compound offered further evidence for the authenticity of the suggested structures.

3.2.2. FTIR

The solid-state infrared spectra of neutral salicylidene-iminothiazole Schiff bases (SITSB) (**4a,b**) and ionic salicylidene-iminothiazole Schiff bases (ISITSB) (**5a-e**) offer preliminary evidences for their successful formation. Moreover, FTIR spectra provide an idea about the possible tautomeric equilibrium for these Schiff bases in the solid state. The prominent features of the FTIR spectra for these Schiff bases are highlighted as follow: (i) A broad band at the range of 3434–3381 cm^{-1} attributed to the stretching vibration of an intramolecular hydrogen-bonded phenolic OH group (O—H···N) within the 2-hydroxybenzylidene-imine segment which is further confirmed by the displacement of the azomethine (—HC═N—) stretching band to lower wavenumber. (ii) Two strong sharp bands at the range of 1621–1606 and 1591–1564 cm^{-1} were assigned to C═N stretching vibrations of azomethine and thiazole moieties which strongly supported the evidence of successful condensation. (v) Interestingly, a very weak shoulder around 1597 cm-1 which could be assigned as a perturbed carbonyl stretching. A significantly lower frequency this vibration than that known for a free carbonyl attributable to the formation of H-bonded six-membered chelate rings in ketoenamine tautomer as shown in Scheme 2. This is indicative of that the central backbone of new aminothiazole Schiff bases is in the expected O-protonated enolimine tautomeric form with a minor contribution of N-protonated ketoenamine tautomeric form, in the solid state. (iv) The medium and sharp band around 1274 cm^{-1} was assigned to the stretching vibration of Ar—O. (v) Medium stretches around 1050 and 740 cm^{-1} are characteristic for asymmetric and symmetric vibrations for ν(C—S—C) of thiazole ring. (vi) The vibrational bands at ~865 and ~770 cm^{-1} are due to the in-plane and out-plane flexible vibrations of the imidazolium ring.

3.2.3. NMR spectroscopy

Examination of the ^{1}H NMR spectra of aminothiazole Schiff bases ((**4a,b**), (**5a-e**)) leads us to highlight the following aspects: (i) The aldehydic proton singlet which was observed at δ = ~10.30 ppm in the ^{1}H NMR spectra of Sal-ILs (**3a-e**) has been lost from the spectra of their corresponding Schiff bases, instead, a new singlet assignable to the resonance of azomethinic (H—C═N) proton was observed around 9.00 ppm. (ii) The resonance of salicylic hydroxyl proton which is a

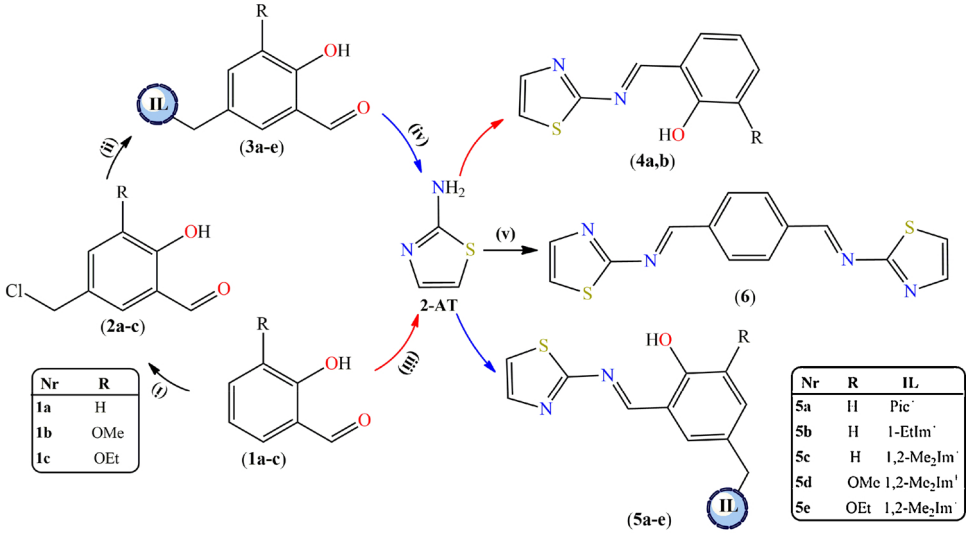

(i) CH_2O, $ZnCl_2$, HCl_{aq}, HCl_g, stir, r.t. **(ii)** 1-EtIm, 1,2-Me_2Im or Pic, toluene, stirr, 60 °C, N_2. **(iii)** **1b** or **1c**, EtOH, reflux. **(iv)** **3a-e**, EtOH, reflux. **(v)** Terephthalaldehyde, EtOH, reflux

Scheme 1. Schematic diagram for the synthesis of Sal-ILs (**3**a-e) and neutral/ ionic SITSB and BBITSB.

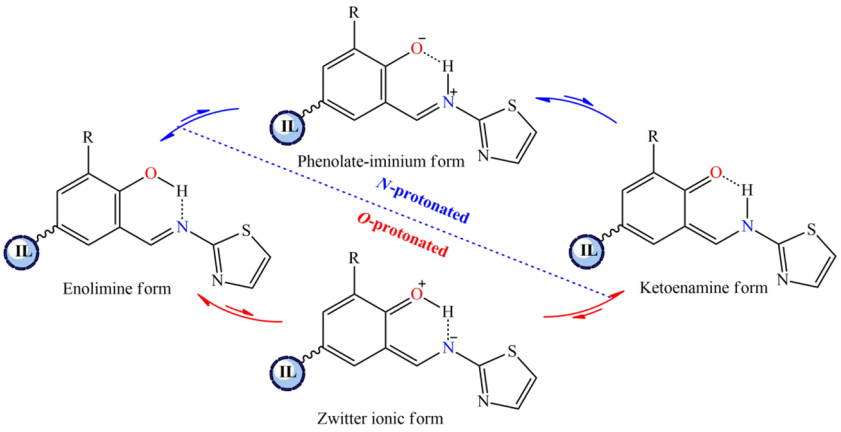

Scheme 2. Possible tautomeric forms and H-bonding profile in aminothiazole Schiff bases ((**4**a,b), (**5**a-e)).

measure of the hydrogen bonding/ transfer ability [28] was observed between 11.36 and 10.27 ppm. (iii) The central salicylidene backbone is in the expected *O*-protonated tautomeric form as revealed from the splitting pattern of azomethinic proton which noticed as a singlet, typical for enolimine tautomeric form, and the downfield shift of phenolic proton signal in all compounds attributable for the intramolecular H-bond to the imine nitrogen (*cf.* Scheme 2). (iv) Interestingly that in the ^{1}HNMR spectrum of (**5e**), the azomethinic proton signal splits into a doublet due to a coupling with the enamine proton. This splitting pattern is characteristic for ketoenamine tautomeric form, in other words, the tautomeric equilibria for deuterated solution of (**5**e) is significantly shifted toward the ketoenamine tautomeric form.

Further evidence for the predominance of *O*-protonated tautomer in new Schiff bases is provided by ^{13}C NMR spectroscopy. Claramunt et al. remarked that the fluctuation of ^{13}C resonance values from ~160 ppm for an enol-imine to ~180 ppm for a pure ketoenamine tautomer [29], making the ^{13}C spectrum a powerful tool to discern the relative enol-imine/ ketoenamine tautomeric population. The ^{13}C NMR spectra of aminothiazole Schiff bases ((**4a,b**), (**5a-e**)) exhibits a resonance at *ca* 160.0 ppm typical for enol-imines tautomer (160.9 ppm). Furthermore, signal around 166 ppm is observed, which can be assigned to the carbons of the aldimine (H−C═N) moieties. Thus, NMR studies of reveal that, the acidic protons of the central salicylidene backbone are bond to O atom and not bond to N atom.

3.3. Antibacterial activity against marine bacterial isolates

Exploring for new antibiofoulants have faced numerous unsuccessful trials due to several reasons including a high cost of fabrication, severe damage to marine communities or short-time effect for the antibiofouling products. Continuing our journey in the exploration of new antibiofouling, we have designed and fabricated new aminothiazole Schiff bases with/ without ionic liquid moieties (**4a,b**, **5a-e**, **6**) with emphasize to obtain new antibiofoulants with potent antibacterial activity.

The target aminothiazole Schiff bases ((**4a,b**), (**5a-e**), **6**) and standard Diuron® were *in vitro* assessed for their biological capacity to inhibit the growth of four significant marine biofilm-inducing bacterial strains including *S. aureus*, *A. hydrophilia*, *E. coli* and *Vibrio*. Noticeable, examination of inhibition zones (Fig. 1) revealed the higher efficacy for most of the tested compounds in comparison to Diuron®, particularly against gram negative bacteria, *E. coli and A. hydrophila*, which have potential capability to grow in water environments and to induce biofilms [30]. Noteworthy, gram negative bacterial cell walls are very complex in their chemistry and their outer membranes structure which composed of lipopolysaccharides layers [31]which are known to have high resistance toward biocides [32].

Among tested compounds, **4b** and **5e** have shown the most effective antibacterial capacity towards *A. hydrophilia*. This inhibitory activity could be attributed to hydrogen bonding (intramolecular /intermolecular) through azomethine group (−HC═N−) with active centers of cell constituents resulting in interference with normal cell processes [33]. Meanwhile, the imidazolium cation, belongs compound (**5e**), is being attracted electrostatically to the phosphate groups of bacterial cell wall [34]. Additionally, the hydrophobic pharmacophore (ethoxy group) in these compounds could enhances their penetration through the lipophilic bacterial cell wall and disrupts the cytoplasmic membrane with simultaneous releasing of bacterium constituents causing pathogen death, eventually[35]. Furthermore, compound (**4a**) exhibited an exceptional higher antibacterial action against *E. coli*.

3.4. Field anti-macrofouling assay at Alexandria Eastern Harbour beach

Although exploring for new anti-biofouling coatings using laboratory based bioassays can be useful, helpful and quite reliable tool to give a preliminary vision about the antifouling performance of these new compounds but the ecological significance of laboratory bioassays appears to be very limited and should be supported by subsequent field experiments. The field experiments give an idea about the durability of these AF coatings under variable conditions including wind, chemical attack of polluted water and biological attack of marine life.

3.4.1. Environmental parameters of Alexandria Eastern Harbour waters

Field static immersion tests were performed from 12th May 2015 to 6th October 2015 (147 days) in Alexandria Eastern Harbor (AEH), Egypt. The change in the environmental parameters in AEH during this study is represented in Fig. 2, where the temperature of surface water samples ranges from 21.70 to 34.00 °C, pH ranges from 7.97 to 8.57, salinities range from 36.90 to 37.80‰, DO level ranges from 2.46 to 6.50 mg O_2/L, dissolved inorganic phosphorus (DIP) level ranges from 0.35 to 1.85 µg/L, nitrate level ranges from 0.06 to 0.50 µg/L, nitrite level ranges from 0.05 to 0.75 µg/L, ammonia level ranges from 0.42 to 0.68 µg/L, silicate level ranges from 1.97 to 5.68 µg/L, sulphate level ranges from 2.57 to 4.53 µg/L and OOM level ranges from 0.16 to 1.60 mg O_2/L. During all seasons, the diversified biofouling comes at most cases from bacteria, tube worms, barnacles, bryozoan and macroalgae colonization.

3.4.2. Field static immersion test

To investigate the antifouling performance of new aminothiazole Schiff bases under harsh natural marine environmental conditions, these Schiff bases were incorporated into the matrix of commercial paint to fabricate new coatings formulations. The prepared coating formulations incorporated most potent compounds (**4a,b**), (**5a-c**), (**6**) and a standard antifoulant (Diuron®), have been applied, separately, to polyacrylic panels and tested for their antibiofouling efficacies, in

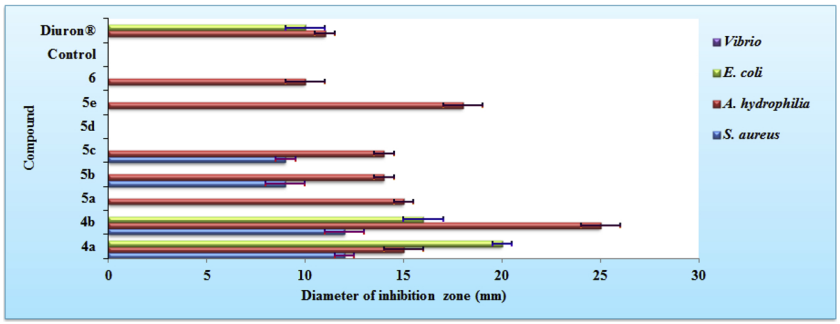

Fig. 1. Graph of mean inhibition zone (mm) for target compounds against different bacterial strains.

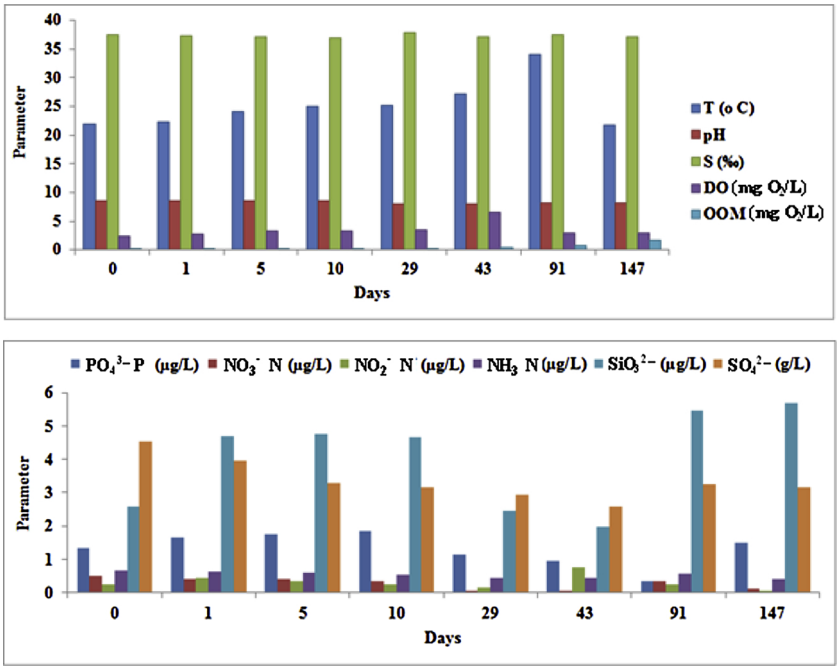

Fig. 2. Environmental parameters of Alexandria Eastern Harbor waters during immersion time.

comparison to blank and control panels, under static and harsh marine conditions in AEH, Mediterranean, Egypt, for 147 days. The attachment of various macrofoulants to the coated, blank and control panels was observed by visual inspection. Fig. 3 shows the photographic images of panels coated with the prepared formulations in comparison to blank and control panels. Fouling development on different coated/ uncoated panels for a period of 147 days was estimated as the cover percentage of various fouling organisms on each submerged panel.

Biofilm formation is the main road for biofouling in most industrial systems. Biofilms could stimulate the settlement and succession of some macrofouling organisms [36] such as algal spores [37] and larvae of tube-worms and barnacles [38]. Results from the present study were collected and outlined in Fig. 4 which demonstrated that compound (**4a**) was found to be the most effective one in fighting slime film (biofilm) formation during the whole experiment duration. Moreover, compounds (**4b**), (**5a-c**) and (**6**) were resistant for the slim film (biofilm) formation for the early 42 days, however on the day 43, biofilms with a coverage percent in the range of 60–90% were developed upon their surfaces which then which then disappeared under the experiment`s conditions after 63 days. These effects may be due to their partial solubility in the seawater [22a]. Another reason could be the effective impact of those compounds on quorum-sensing, a process responsible for bacterial cells communication, and signal substances such as *N*-acyl homoserine lactones (AHLs) which is essential in govern population density-dependent behaviors [39].

Algae are a large and diverse group of simple autotrophic macrofouling organisms [40]. During our study, it is noticed that the growth of brown and red algae upon coated panels have significantly influenced by the seawater environmental parameters as their normal growth was suddenly decreased after 91 days. This could be ascribed to a lower seawater temperature [41] ($r = 0.80$ for brown algae) and nutrients concentration ($r = 0.65$ (NH_3-N) and $r = 0.79$ (NO_2^--N) (see Fig. 5) which are crucial factors for the growth of brown and red macroalgae. Noteworthy, all compounds exhibited different resisting profiles toward brown algae: for example, compound (**6**) has fully inhibited the colonization of brown macro-algae on its panel which exhibited no growth of brown macro-algae during the whole experiment duration. A panel coated by **4a**-formulation exhibited little coverage of brown macro-algae which were completely detached after 43 days. On the other hand, compounds (**4b**) and (**5a-c**) showed moderate ability to prevent the attachment of macro-algae on their panels surfaces as revealed from the observed densities of macro-algae upon their panels which ranged between 30 and 55% during a period of 43–63 days, however, macro-algae were completely disappeared after 63–91 days in spite of a 60% brown algal coverage percent observed on the blank panel after 91 days. Furthermore, moderate to higher densities of green macro-algae with a coverage percent in the range of 20–90% were observed on the surfaces of panels coated with compounds (**4a,b**), (**5a-c**) and (**6**) during the first 29 days, but fortunately, these macro-algae were completely disappeared after 91 days. Moreover, most of the

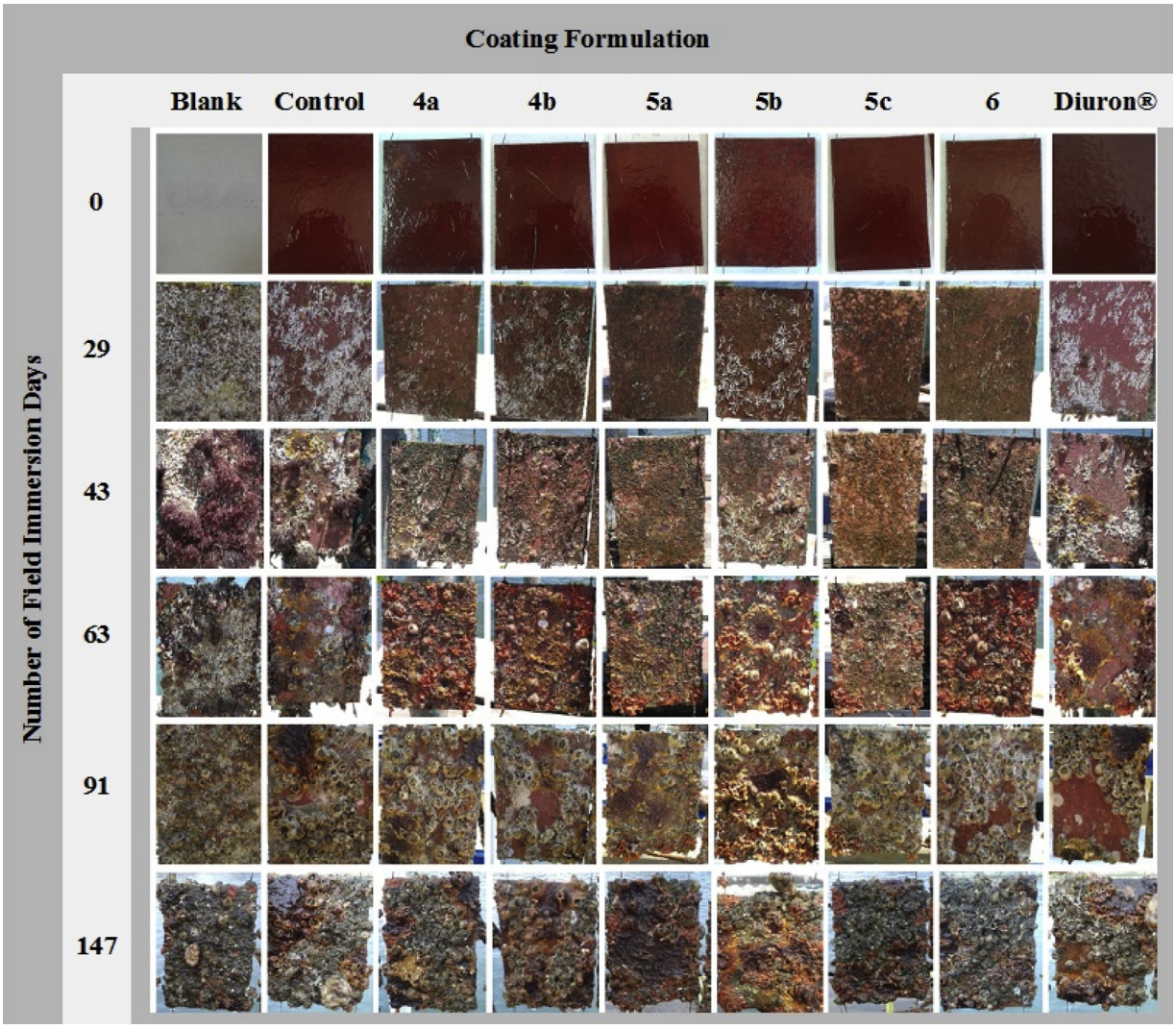

Fig. 3. Photographs showed the visual appearance of panels coated with formulations incorporated compounds (**4a,b**), (**5a-c**) and (**6**), in comparison to control- & Diuron®-coated and uncoated panels. These photographs were taken during performing field static immersion test at Alexandria Eastern Harbor, Mediterranean sea, Egypt. The 'Control' panel was coated with the paint formulation without any aminothiazole derivatives.

tested compounds were good retardants for the colonization of red macro-algae, better than Diuron®, during all experiment duration (*cf.* Fig. 5). Accordingly, the unique resisting profile against algal colonization noticed for most compounds confirmed their validity as anti-macro-algal additives in the formulation of antifouling coatings.

Tube-worms and barnacles are of the most dominant fouling species in AEH [22a]. These macrofoulants produce hard calcium carbonate exoskeleton tubes which give them protection against predators [42] and pathogens [43]. These hard exoskeletons need special electrical machines to remove them from ship's hull *i.e.* expensive cleaning tools. Noticeable, after a period of 29 days of immersion in AEH, the control, blank and Diuron® coated panels were heavily fouled with tube-worms and barnacles. The coverage percent of tube-worms and barnacles upon these panels were initially reached to 95% and 20% and have increased to 100% and 65% after 147 days, respectively. This clarified that Diuron® showed no resistance at all towards tube-worms. It is well known that, settlement of tube-worms and barnacles is promoted by finding nutrition sources essential for initiation of phytoplankton blooms which support their colonization [44]. So, this high fouling pressure of tube-worms and barnacles could be attributed to the high levels of nutrients and organic matter observed at this immersion site [r = 0.60 (PO_4^{3-}-P), r = 0.75 (SiO_3^{2-}-Si), r = 0.92(OOM)] and [r = 0.70 (NO_3^--N), r = 0.90 (SiO_3^{2-}-Si), r = 0.81 (OOM)] (see Fig. 5) for tube-worms and barnacles, respectively.

Contrary, compounds (**5a,b**) exhibited good resistance to tube-worms growth, in spite of high fouling pressure, they showed only little densities of tube-worms (6–10%) after 147 days. Also, compounds (**4a,b**) were better than Diuron® in fighting the colonization of tube-worms as their panels colonized by 15–20% of tube-worms after 147 days.

Compounds (**4b**) and (**5a,b**) exhibited higher efficiencies than Diuron® towards barnacle colonization, their panels showed very little densities, not exceed 3%, of living barnacles after 147 days. Also, compound **4a** have the ability to hinder the growth of living barnacle more than Diuron® so that the coverage percent of barnacle on its panel not exceed 10% after 147 days.

Bryozoan, ascidians and zooids growth is mainly affected by nutrient concentrations and OOM. Although, significant strong positive correlations have been noticed between the level of nitrate, silicate and OOM concentrations with the coverage percent of bryozoan, ascidian and zooids as shown in (Fig. 5). For instance, compounds (**4b**) (colonized bryozoans/ 147 days = 20%) and (**6**) (colonized bryozoans/ 147 days = 25%) have inhibited the settlement of bryozoans, more efficiently than Diuron®, which showed no inhibitory effect at all. Contrarily, compound (**5c**) (colonized bryozoans/ 147 days = 40%) showed weak resistance against the growth of bryozoans. Furthermore, all compounds were good retardants for ascidians and zooids, growth during the whole experiment duration.

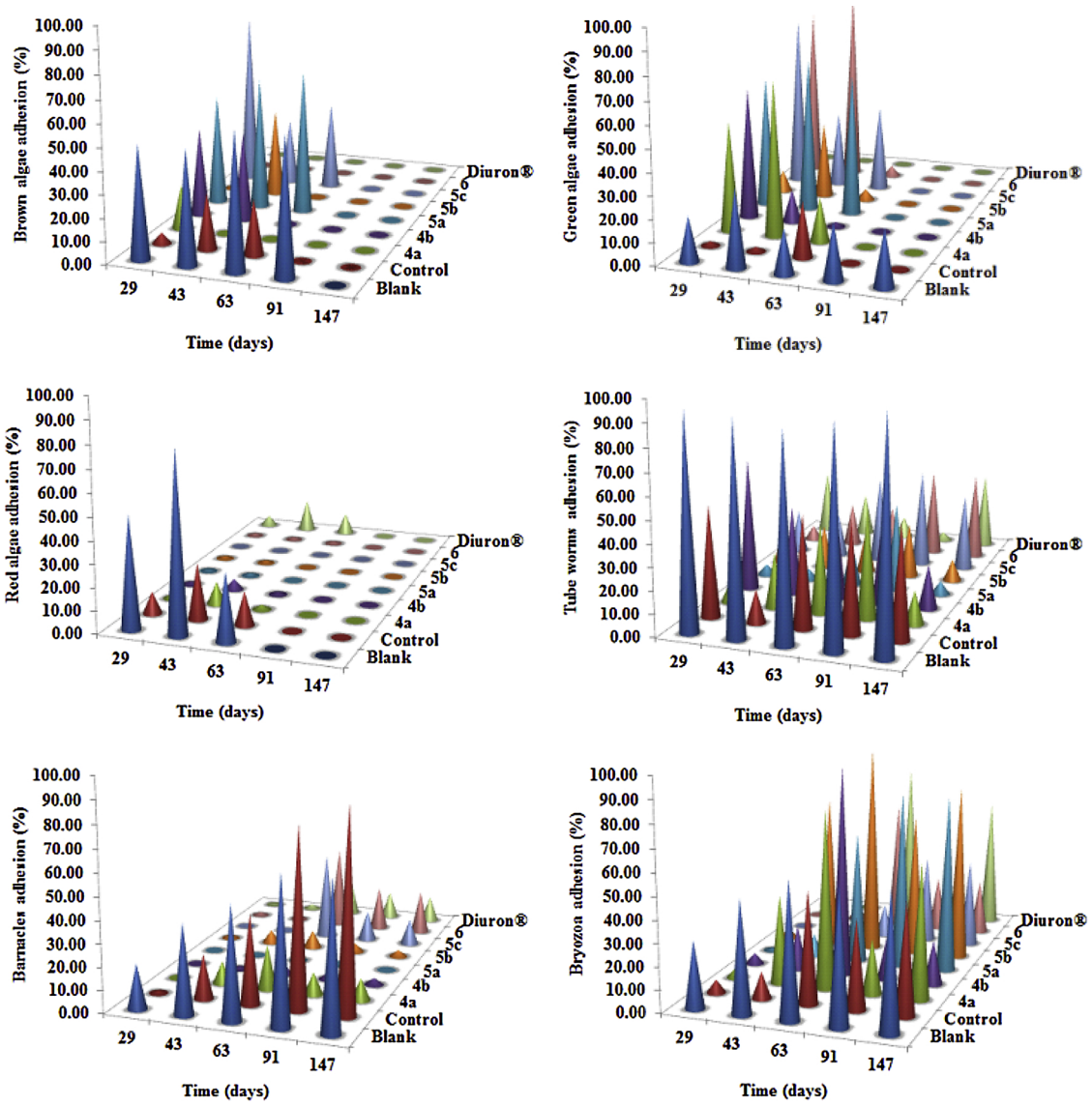

Fig. 4. Coverage percent of different marine fouling organisms during experiment duration for blank, control and coated acrylic panels immersed in Alexandria Eastern Harbor starting from 12 May 2015 to 6 October 2015.

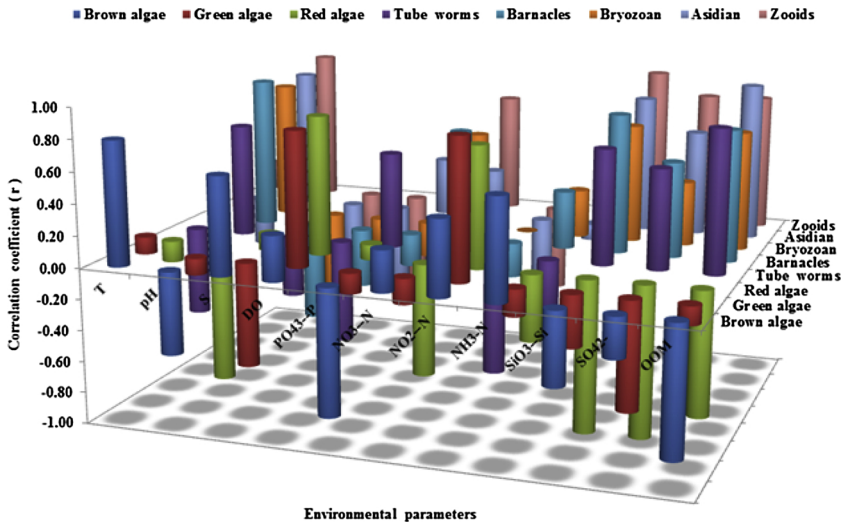

Fig. 5. Correlation coefficient (r) between environmental parameters and normal growth coverage percent of marine fouling organisms.

4. Conclusion

Our work demonstrates varied synthetic strategies to prepare salicylidene-iminothiazole (SITSB) and benzylidene-bis-iminothiazole (BBITSB) Schiff bases. Biological assessment of new compounds revealed higher antibacterial efficacies than Diuron®, a standard antifoulant, especially against gram negative bacteria, *A. hydrophila* and *E. coli*. Compounds (**4b**) and (**5e**) were found to be the most effective towards *A. hydrophilia*. While compound (**4a**) was the most effective against *E. coli*.

The prepared compounds have incorporated into the matrix of inert coating formulations which applied to polyacrylic panels and subjected to a field static immersion study, for antibiofoling assay. This study demonstrated that major of the tested coating formulations exhibited significant antibiofouling efficacy under harsh marine conditions in comparison to that containing a standard antifoulant, Diuron®. In summary. All compounds have remarkable efficacy to inhibit the biofilm formation, colonization of macro-algal and growth of ascidians and zooids, as well. Moreover, compounds (**5a,b**) exhibited highest efficiency against the settlement of tube-worms upon the surface of their panels. Additionally, compounds (**4b**) and (**5a,b**) showed highest efficiency towards colonization of barnacle. Finally, compounds (**4b**) and (**6**) are the most active against fouling with bryozoans.

Appendix A. Supplementary data

Supplementary material related to this article can be found, in the online version, at doi:https://doi.org/10.1016/j.jece.2018.11.044.

References

[1] I. Fitridge, T. Dempster, J. Guenther, R. Nys, The impact and control of biofouling in marine aquaculture: a review, Biofouling 28 (2012) 649–669.

[2] S. Cao, J. Wang, H. Chen, D. Chen, Progress of marine biofouling and antifouling technologies, China Sci. Bull. 56 (2011) 598–612.

[3] J.W. Costerton, P.S. Stewart, E.P. Greenberg, Bacterial biofilms: a common cause of persistent infections, Science 284 (1999) 1318–1322.

[4] H. Lee, D.H. Kim, J. Cho, S. Moon, Characterization of anion exchange membranes with natural organic matter (NOM) during electrodialysis, Desalination 151 (2003) 43–52.

[5] Y.T. Cui, S.L.M. Teo, W. Leong, C.L.L. Chai, Searching for "environmentally-benign" antifouling biocides, Int. J. Mol. Sci. 15 (2014) 9255–9284.

[6] A.A. Chavan, N.R. Pai, Synthesis and antimicrobial screening of 5-arylidine-2-imino-4-thiazol-idinones, Arkivoc 14 (2007) 148–155.

[7] G. Wells, T.D. Bradshaw, P. Diana, A. Seaton, D.F. Shi, A.D. Westwell, The synthesis and antitumour activity of benzothiazole substituted quinol derivatives, Bioorg. Med. Chem. Lett. 10 (2000) 513–515.

[8] (a) T. Akhtar, S. Hameed, N.A. Al-Masoudi, *In vitro* antitumor and antiviral activities of new benzothiazole and 1,3,4-oxadiazole-2-thione derivatives, Acta Pharm. 58 (2008) 135–149;
(b) V. Javali, E. Jayachandrane, R. Shah, K. Patel, G.M. Sreenivasa, Synthesis, characterization and anthelmintic activity (perituma- posthuma) of fluoro substituted benzothiazole for biological and pharmacological screening, Int. J. Pharma Bio Sci. 1 (2010) 1–8.

[9] S.R. Pattan, C.H. Suresh, V.D. Pujar, V.V.K. Reddy, V.P. Rasal, B.C. Koti, Synthesis and antidiabetic activity of 2-amino [5'(4-sulphonylbenzylidine)- 2,4-thiazolidinedione]-7-chloro-6-flourobenzothiazole, Indian, J. Chem. Sect. B 44 (2005) 2404–2408.

[10] B.S. Dawane, S.G. Konda, A versatile multicomponent one-pot synthesis of Thiazole derivatives under solvent free conditions: designed by pass showed antiviral activity as predicted, Int. J. Pharm. Sci. Rev. Res. 3 (2010) 96–98.

[11] M.S. Pingle, Synthesis and biological activity of 4H-pyrimido [2,1-b]benzothiazole-8-substituted-2-thiomethyl-3-cyano-4-ones, Indian J. Heterocy. Chem. 12 (2003) 343–346.

[12] F.A. Hassan, Synthesis, characterization, anti-inflammatory, and antioxidant activities of some new thiazole derivatives, Int. J. App. Sci. Tech. 2 (7) (2012) 180–187.

[13] S. Rollas, S.G. Kucukguzel, Biological activites of hydrazone derivatives, Molecules 12 (2007) 1910–1939.

[14] V. Javali, E. Jayachandrane, R. Shah, K. Patel, G.M. Sreenivasa, Synthesis, characterization and anthelmintic activity (perituma- posthuma) of fluoro substituted benzothiazole for biological and pharmacological screening, Int. J. Pharma Bio Sci. 1 (2010) 1–8.

[15] M.M. Abd-Elzaher, A.A. Labib, H.A. Mousa, S.A. Moustafa, M.M. Ali, A.A. El-Rashedy, Synthesis, anticancer activity and molecular docking study of Schiff base complexes containing thiazole moiety, Beni-Suef University, J. Bas. App. Sci. 5 (2016) 85–96.

[16] F. Azam, S. Singh, S.L. Khokhra, O. Prakash, Synthesis of Schiff bases of naphtha [1,2-*d*]thiazol-2-amine and metalcomplexes of 2-(2'-hydroxy) benzylidene amino naphthothiazole as potential antimicrobial agents, J. Zhejiang Univ. Sci. B 8 (2007) 446–452.

[17] Z.H. Chohan, M. Arif, M.A. Akhtar, C.T. Supuran, Metal-based antibacterial and antifungal agents: synthesis, characterization, and in vitro biological evaluation of Co(II), Cu(II), Ni(II), and Zn(II) complexes with amino acid-derived compounds, Bioinorg. Chem. App. (2006) 1–13.

[18] (a) R.F.M. Elshaarawy, C. Janiak, Ionic liquid-supported chiral saldach with tunable hydrogen bonding: synthesis, metalation with Fe(III) and in vitro antimicrobial susceptibility, Tetrahedron 70 (2014) 8023–8032;
(b) R.F.M. Elshaarawy, Z.H. Kheiralla, A.A. Rushdy, C. Janiak, New water soluble bis-imidazolium salts with a saldach scaffold: synthesis, characterization and in vitro cytotoxicity/ bactericidal studies, Inorg. Chim. Acta Rev. 421 (2014) 110–122;
(c) R.F.M. Elshaarawy, C. Janiak, Toward new classes of potent antibiotics: synthesis and antimicrobial activity of novel metallosaldach–imidazolium salts, Eur. J. Med. Chem. 75 (2014) 31–42;
(d) K.S. Egorova, V.P. Ananikov, Toxicity of ionic liquids: eco(cyto)activity as complicated, but unavoidable parameter for task-specific optimization, Chem. Sus. Chem. 7 (2014) 336–360;
(e) J. Yu, S. Zhang, Y. Dai, X. Lu, Q. Lei, W. Fang, Antimicrobial activity and cytotoxicity of piperazinium- and guanidinium-based ionic liquids, J. Hazard. Mater. 307 (2016) 73–81.

[19] (a) H.-L. Chen, H.-F. Kao, J.-Y. Wang, G.-T. Wei, Cytotoxicity of imidazole ionic liquids in human lung carcinoma A549 cell line, J. Chin. Chem. Soc. (Weinheim, Ger.) 61 (2014) 763–769;
(b) V. Malhotra, V. Kumar, C. Velez, B. Zayas, Imidazolium-derived ionic salts induce inhibition of cancerous cell growth through apoptosis, Med. Chem. Res. 5 (2014) 1404–1409.

[20] S. Anvari, H. Hajfarajollah, B. Mokhtarani, M. Enayati, A. Sharifi, M. Mirzaei, Antibacterial and anti-adhesive properties of ionic liquids with various cationic and anionic heads toward pathogenic bacteria, J. Mol. Liq. 221 (2016) 685–690.

[21] (a) R.F.M. Elshaarawy, T.B. Mostafa, A.A. Refaee, E.A. El-Sawi, Ionic Sal-SG Schiff bases as new synergetic chemotherapeutic candidates: synthesis, metalation with Pd(II) and in vitro pharmacological evaluation, RSC Adv. 5 (2015) 68260–68269;
(b) R.F.M. Elshaarawy, C. Janiak, Antibacterial susceptibility of new copper(II)N-pyruvoyl anthranilate complexes against marine bacterial strains – in search of new antibiofouling candidate, Arab. J. Chem. 9 (2016) 825–834.

[22] (a) R.F.M. Elshaarawy, F.H.A. Mustafa, L.V. Geelen, A.E.A. Abou-Taleb, H.R.Z. Tadros, R. Kalscheuer, C. Janiak, Mining marine shell wastes for polyelectrolyte chitosan anti-biofoulants: Fabrication of high-performance economic and ecofriendly anti-biofouling coatings, Carbohydr. Polym. 172 (2017) 352–364;
(b) R.F.M. Elshaarawy, F.H.A. Mustafa, A. Herbst, A.E.M. Farag, C. Janiak, Surface functionalization of chitosan isolated from shrimp shells, using salicylaldehyde ionic liquids in exploration for novel economic and ecofriendly antibiofoulants, RSC Adv. 6 (2016) 20901–20915.

[23] C. Perez, M. Paul, P. Bazerque, An antibiotic assay by the agar well diffusion method, Acta Bio. Med. Exp. 15 (1990) 113–115.

[24] K. Grasshoff, Methods of Seawater Analysis, Verlage Chemie Weinkeim, New York, 1976.

[25] Food and Agriculture Organization of the United Nations [FAO], Permanganate Value of Organic Matter in Natural Waters, Fisheries Technical Paper 137 (1975), pp. 169–171.

[26] T.R. Parsons, Y. Maita, C.M. Lalli, A Manual of Chemical and Biological Methods for Seawater Analysis, Pergamon Press, 1984.

[27] J.R. Rossum, P.A. Villarruz, Suggested methods for turbidimetric determination of sulphate in seawater, J. Am. Water Works Assoc. 53 (1961) 873–887.

[28] (a) M. Tuncel, S. Serin, Synthesis and characterization of Copper(II), Nickel(II) and Cobalt(II) complexes with azo-linked schiff base ligands, Synth. React. Inorg. Met.-Org. Nano-Met. Chem. 35 (2005) 203–212;
(b) W. Kemp, NMR in Chemistry: A Multinuclear Introduction, 1st ed., Macmillan Education Ltd., London, 1986, pp. 57–59.

[29] R.M. Claramunt, C. López, M.D. Santa María, D. Sanz, J. Elguero, The use of NMR spectroscopy to study tautomerism, Prog. Nucl. Magn. Reson. Spectrosc. 49 (2006) 169–206.

[30] C. Chauret, C. Volk, R. Creason, J. Jarosh, J. Robinson, C. Warnes, Detection of *Aeromonas hydrophila* in a drinking water distribution system: a field and pilot study, Can. J. Microbiol. 47 (2001) 782–786.

[31] M.R.J. Salton, J.G. Pavlik, Studies of the bacterial cell wall VI. Wall composition and sensitivity to lysozyme, Biochim. Biophys. Acta 39 (1960) 398–407.

[32] A.D. Russell, Similarities and differences in the responses of microorganisms to biocides, J. Antimicrob. Chemother. 52 (2003) 750–763.

[33] L.H.Abdel Rahman, A.M. Abu-Dief, N.A. Hashem, A.A. Seleem, Recent advances in synthesis, characterization and biological activity of nano sized schiff base amino acid m(II) complexes, Int. J. Nano. Chem. 1 (2015) 79–95.

[34] Z. Zheng, Q. Xu, J. Guo, J. Qin, H. Mao, B. Wang, F. Yan, Structure – Antibacterial activity relationships of imidazolium-type ionic liquid monomers, poly(ionic liquids) and poly(ionic liquid) membranes: effect of alkyl chain length and cations, ACS Appl. Mater. Interfaces 8 (2016) 12684–12692.

[35] R.F.M. Elshaarawy, H.R.Z. Tadros, R.M. Abd El-Aala, F.H.A. Mustafa, Y.A. Soliman, M.A. Hamed, Hybrid molecules comprising 1,2,4-triazole or diaminothiadiazole Schiff-bases and ionic liquid moieties as potent antibacterial and marine anti-biofouling nominees, J. Environ. Chem. Eng. 4 (2016) 2754–2764.

[36] C.E. Zobell, E.C. Allen, The significance of marine bacteria in the fouling of submerged surfaces, J. Bacteriol. 29 (1935) 239–251.

[37] K. Marshall, I.R. Joint, M.E. Callow, J.A. Callow, Effect of marine bacterial isolates on the growth and morphology of axenic plantlets of the green alga ulva linza, Microb. Ecol. 52 (2006) 302–310.
[38] J.D. Zardus, B.T. Nedved, Y. Huang, C. Tran, M.G. Hadfield, Microbial biofilms facilitate adhesion in biofouling invertebrates, Biol. Bull. 214 (2008) 91–98.
[39] M. Teplitski, J.B. Robinson, W.D. Bauer, Plants secrete substances that mimic bacterial N-Acyl homoserine lactone signal activities and affect population density-dependent behaviors in associated bacteria, Mol. Plant Microbe Interact. 13 (2000) 637–648.
[40] M. Salta, L. Chambers, J. Wharton, R. Wood, J.F. Briand, Y. Blache, K. Stokes, Marine fouling organisms and their use in antifouling bioassays, Conference: EUROCORR 6 (2009).
[41] A.I. Sousa, I. Martins, A.I. Lillebø, M.R. Flindt, M.A. Pardal, Influence of salinity, nutrients and light on the germination and growth of Enteromorpha sp. Spores, J. Exp. Mar. Biol. Ecol. 341 (2007) 142–150.
[42] C.E. Kicklighter, M.E. Hay, To avoid or deter: interactions among defense strategies in sabellid worms, Oecologia 151 (2007) 161–173.
[43] F.H. Wilt, C.E. Killian, B.T. Livingston, Development of calcareousskeletal elements in invertebrates, Differentiation 71 (2003) 237–250.
[44] J.P. Ryan, J.B.J. Harvey, Y. Zhang, C.B. Woodson, Distributions of invertebrate larvae and phytoplankton in a coastal upwelling system retention zone and peripheral front, J. Exp. Mar. Biol. Ecol. 459 (2014) 51–60.